HIGH PRESSURE RAMAN STUDY OF SOLUBILIZED SINGLE WALLED CARBON NANOTUBES

U. Schlecht[1], U. D. Venkateswaran [2], E. Richter [3], J. Chen[4], R. C. Haddon[5], P. C. Eklund[6] and A. M. Rao [7]

[1]Max-Planck Institute for Solid State Research, 70569 Stuttgart, Germany
[2]Department of Physics, Oakland University, Rochester, MI 48309
[3]Department of Physics & Astronomy, University of Kentucky, Lexington, KY 40506
[4]Zyvex Corporation, Richardson, TX 75081
[5]Department of Chemistry, University of California, Riverside, CA 92521
[6]Department of Physics, Pennsylvania State University, University Park PA 16802,
[7]Department of Physics and Astronomy, Clemson University, Clemson, SC 29634

Introduction

The study of Raman-active modes in single walled carbon nanotubes (SWNTs) as a function of external pressure has been used to determine the influence of van der Waals (vdW) interactions on the vibrational modes in SWNTs [1-5], and to investigate pressure-induced structural transitions in SWNTs [3,5]. Recently, pressure induced changes in the electrical [6] and optical [7] properties of SWNTs have also been reported. Two widely used methods to synthesize SWNTs are the electric arc (EA) [8] and pulsed laser vaporization (PLV) [9] methods which produce crystalline "ropes" or "bundles" consisting of ~100 SWNTs held together in a triangular lattice by vdW forces. From the transmission electron microscopy and x-ray diffraction measurements, a typical SWNT bundle produced by PLV or the EA method is found to consist of tubes whose diameters vary by ~0.2 nm around the most dominant tube diameter d_o ~1.4 nm.

Raman spectroscopy has evolved into a useful and convenient characterization tool for pristine and doped SWNTs. A typical Raman spectrum of SWNT bundles collected at ambient pressure using 1064 nm excitation exhibits two prominent bands at ω_R ~160 cm^{-1} (radial band) and ω_T ~1590 cm^{-1} (tangential band). The position of these bands is sensitive to excitation wavelength [10], external pressure[1-5], dopant type [11], size of the bundle [12], and the tube diameter [10,13]. A carbon nanotube can be viewed as a graphene sheet rolled into a seamless tube with a chiral vector $C = n\mathbf{a}_1 + m\mathbf{a}_2$, where n and m are integers and $\mathbf{a}_1$ and $\mathbf{a}_2$ are the primitive lattice vectors for a graphene sheet. For a fixed value of (n, m), a single radial mode with A_{1g} symmetry and three tangential modes with A_{1g}, E_{1g} and E_{2g} symmetries (six modes with A_1, E_1 and E_2 symmetries) are expected for achiral (chiral) tubes [14]. While the frequency of the tangential mode are nearly independent of the tube diameter, the radial mode frequency depends inversely on the tube diameter [14].

The first detailed experimental and theoretical investigation of the pressure

dependence of Raman modes in SWNT bundles were reported by Venkateswaran et al [1]. Different pressure dependences for ω_R were predicted by a generalized tight binding molecular dynamic (GTBMD) simulation for bundled and isolated tubes. The experimental data in Ref. 1 was best described by the GTBMD calculation in which the pressure medium resides outside the bundle and exerts a uniform hydrostatic pressure on the bundle, i.e., the pressure medium does not penetrate into the interstitial channels of the bundle. In this paper, we report the experimental pressure dependences of ω_R and ω_T for nearly isolated, or small SWNT bundles containing 1-7 SWNTs, and compare them to those predicted by the GTBMD calculations.

Experimental Details

Chemical methods have been developed which allow as-prepared SWNT bundles to be processed into smaller bundles (containing 1-7 tubes) that are soluble in organic solvents such as, CS_2 and THF [15]. Details of the preparation and characterization of the solubilized tubes (S-SWNTs) are described in Ref. 15. The S-SWNT samples were obtained in the solid form by evaporating the solution in which they were dissolved. A sample of S-SWNT in powder form (~ 0.10 x 0.10 mm^2) and a tiny ruby crystal were loaded into a diamond anvil cell using a mixture of four volume parts of methanol with one volume part of ethanol as the pressure transmitting medium. Raman data were obtained at elevated pressures in the range of 0 – 4.7 GPa using the 514.5 nm laser excitation, and a HR 460 spectrometer equipped with a liquid nitrogen cooled CCD (ISA Instruments). The 546.07 nm emission line from a mercury source was used to calibrate the spectrometer while the frequency positions of the ruby luminescence lines were used to calibrate the pressure.

Results and discussion

In the GTBMD scheme, a Lennard- Jones type potential was used to describe the vdW forces in SWNT bundles using parameters similar to those needed to simulate the c-axis bonding in bulk graphite. The hydrostatic pressure was introduced through a radial force Fp = P. A, where A is a cross sectional area, perpendicular to the tube axis [1]. Three scenarios in which the applied pressure can be transmitted to the sample were considered and are shown schematically in Fig. 1 [1]. In model I, the pressure transmitting liquid resides external to the SWNT bundle and pressure is transmitted only to the outer tubes, and the tubes in the bundle are coupled through vdW forces. Contrary to this scenario, Model II describes a situation in which the pressure transmitting liquid is allowed to penetrate the bundle and exert uniform pressure to individual tubes within the bundle. However, in Model II, the vdW interactions were neglected. This model is expected to describe the pressure dependence of ω_R and ω_T in isolated tubes, where the pressure transmitting liquid can access each tube and van der Waals forces are strongly reduced. Finally, Model III is identical to Model II with the additional constraint that the vdW interactions are included in the GTBMD calculations. The GTBMD calculations showed that the pressure dependence for ω_R was particularly sensitive to the coupling between the tubes in the SWNT bundles. To investigate this effect further, we

determined experimentally the pressure dependence for ω_R and ω_T in S-SWNTs and compare them to the corresponding results obtained previously for bundled SWNTs.

The experimentally determined pressure dependence for ω_R and ω_T in S-SWNT is shown in Figs 2a and 2b, respectively. For increasing pressure, the radial and tangential bands are found to be upshifted in frequency with a concomitant decrease in band intensities. The radial band could not be detected above ~3 GPa. Due to the broadness of radial and tangential bands in Fig. 1, only one and two Lorenztians, respectively, were sufficient to determine the peak positions for these bands. In Figs. 3a and 3b, we compare respectively, the pressure dependence of the radial and tangential bands for S-SWNTs (indicated by squares) obtained in this work to those reported previously in Ref. 1 for bundled SWNTs (indicated by triangles). The solid lines represent fits to the experimental data while the dashed curves represent theoretical pressure dependences for ω_R and ω_T in Models I- III. At least three observations can be made from the data in Figs. 3a and 3b: (i) the slope of the linear fits to ω_R data is similar in both bundled SWNTs and S-SWNTs, (ii) ω_R in S-SWNTs is higher in frequency by ~ 5 cm^{-1} relative to ω_R in bundled SWNTs over the entire pressure range, and (iii) pressure dependences of ω_T in S-SWNTs and bundled tubes is nearly same and ω_T data in S-SWNTs are lower in frequency by ~5 cm^{-1} relative to those in bundled tubes.

The GTMD calculations predict distinct pressure dependences for ω_R in bundled (Model I) and isolated tubes (Model II) (Fig. 3a). The experimental observation of similar pressure dependences for ω_R data in Fig. 3a suggests that a large fraction of the S-SWNT sample contains small bundles rather than isolated tubes. The pressure dependence of ω_R in S-SWNTs is ~ 8.4 cm^{-1}/GPa and is comparable to ~ 9.7 cm^{-1}/GPa observed for ω_R in bundled materials. This experimental observation does not agree with the predicted pressure dependence of ~ 1.3 cm^{-1}/GPa for ω_R in isolated tubes. Interestingly, observation (ii) mentioned above is in contradiction to the expected upshift in ω_R in bundled tubes and could not be understood until recently. At ambient pressure, an anomalous10 cm^{-1} upshift for ω_R in S-SWNTs was observed using 1064, 647.1 and 514.5 nm excitations [12]. It has been suggested that this anomalous upshift arises due to the resonant nature of Raman scattering in SWNTs, and an increased energy gap in the van Hove singularity pairs in bundled tubes relative to the corresponding values in nearly isolated tubes [12]. Further details about this anomalous upshift for ω_R in S-SWNTs can be found in Ref. 12. For completeness, it should be mentioned, that we do not incorporate the shift of resonance in the following discussion. Further theoretical work is needed to determine the effect of high pressure on the electronic density of states in carbon nanotubes.

Returning to Figs. 3a and 3b, we note that the ~ 5 cm^{-1} upshift in ω_R for S-SWNTs is small relative to the 10 cm^{-1} upshift reported for S-SWNTs in Ref. 12. This discrepancy is tentatively attributed to the fact that the S-SWNTs and bundled SWNTs used in this study were obtained from different batches of PLV synthesized SWNTs. In the work described in Ref. 12, all data were obtained on bundled and S-

SWNTs obtained from the same EA or PLV starting material. Furthermore, in an independent study, it was recently discovered that the initially positive values for thermopower in air exposed SWNT bundles become negative when the SWNT bundles are degassed at 500 K in10^{-7} Torr [16, 17]. The tangential band frequency for the degassed bundle was found ~1590 cm^{-1} compared to 1593 cm^{-1} reported previously for air exposed bundles [10]. Negligible change in ω_T for bundled and S-SWNTs was reported in Ref. 12. However, in Fig. 3b, the ω_T data for S-SWNT and bundled SWNTs differ by 5 cm^{-1} [effect (iii) mentioned above] and this inconsistency is also attributed to the different batches of SWNTs used in this study. Regardless, the data obtained in this work can be used to determine the influence of vdW forces on the normalized derivative for ω_R in S-SWNTs as described below.

For a meaningful comparison of the results presented in this work to those already published in the literature, the normalized derivative of ω_R with respect to pressure are listed in Table I. Thomsen et al. [4] used an elasticity model in which a single nanotube is assumed to be a hollow cylinder with a finite wall thickness and isotropic elastic properties. From a comparison of strain components in the axial and tangential directions they estimate the normalized pressure coefficient $\omega_R^{-1}.d\omega_R/dP$ for the radial mode to be twice as high as that for the tangential mode. The tangential direction is defined as the direction that is perpendicular to the tube axis and the radial direction. However, the measured ratio for the radial to tangential normalized pressure coefficients was found to be ~16 [4]. This observation of enhanced value for the ratio led them to suggest that the large pressure coefficient for the radial mode in bundled tubes stems from two contributions: the "pure" radial breathing eigen mode plus a vdW force induced contribution, thus

$$\frac{d\ln\omega_R}{dP} = (1-\alpha)\frac{d\ln\omega_{RBM}}{dP} + \alpha\frac{d\ln\omega_{vdW}}{dP} \qquad (1)$$

α is a measure of the vdW contribution to the pressure derivative [4]. Using the known elastic properties of graphite in equation 1, Thomsen et al. obtained $\alpha \sim 37$ % for bundled SWNTs suggesting that about 37 % of the pressure coefficient for the radial mode arises due to the inter-tube interactions [4]. Values of 3.0 $(TPa)^{-1}$ and 150 $(TPa)^{-1}$ were used for $(d\ln\omega_{RBM}/dP)$ and $(d\ln\omega_{vdW}/dP)$, respectively [4]. A value of 28% was obtained for α in the S-SWNT sample used in this study.

As expected, the value for α in the S-SWNT sample is lower than 37% since the atomic force microscopy images of the S-SWNT sample indicate that a mixture of small bundles with varying diameters exist in the sample. In other words, a solubilized tube can have zero (isolated tubes), two (in a bundle of 3 tubes), three (peripheral tube in a bundle of 7) or six neighbors (center tube in a bundle of 7) as depicted schematically in Fig. 4. The presence of these small ropes along with the isolated tubes in S-SWNT sample may be responsible for the relatively large value of 28% for α.

Conclusions

We performed high pressure Raman experiments on solubilized nanotubes in the pressure range from 0 – 4.7 GPa. The

upshift in ω_R for S-SWNTs relative to ω_R in bundled tubes is attributed to a decreased energy spacing of the van Hove singularities in S-SWNTs over the corresponding spacings in a bundle, thereby allowing the same laser excitation to excite different diameter tubes in these two samples. The relatively high value for $\alpha \sim 28\%$ in S-SWNTs, and the identical pressure dependences for ω_R and ω_T in S-SWNTs and bundled tubes collectively suggest that the solubilized sample contains predominantly small bundles of SWNTs rather than isolated tubes.

Acknowledgements

AMR and RCH acknowledge financial support from the NSF MRSEC grant No. 9809686 and PCE through the NSF MRSEC grant No. 9809686 and ONR grant # N00014-99-1-0619). UDV acknowledges partial support of this research by the Donors of The Petroleum Research Fund, administered by the American Chemical Society. US acknowledges a scholarship from the Fulbright-Commission.

References

1) U.D. Venkateswaran, A.M. Rao, E. Richter, M. Menon, A. Rinzler, R.E. Smalley and P.C. Eklund *Phys. Rev. B* **59**, 10928 (1999).

2) U. D. Venkateswaran, E. A. Brandsen, U. Schlecht, A. M. Rao, E. Richter, I. Loa, K. Syassen and P. C. Eklund, *Phys. Stat. Sol. (b)* **223**, 225 (2001).

3) A. K. Sood et al., *Phys. Stat. Sol. (b)* **215**, 393 (1999).

4) C. Thomsen et al., *Appl. Phys. A* **69**, 309 (1999); S. Reich et al., *Phys. Rev. B* **61**, R13389 (2000).

5) M. J. Peters et al., *Phys. Rev. B* **61**, 5939 (2000).

6) R. Gaal, J. –P. Salvetat and L. Forro, *Phys. Rev. B* **61**, 7320 (2000).

7) S. Kazaoui et al., *Phys. Rev. B* **62**, 1643 (2000).

8. C. Journet et al., Nature **388**, 756 (1997).

9) A. Thess et al., *Science* **273**, 483 (1996).

10) A. M. Rao, E. Richter, S. Bandow, B. Chase, P.C. Eklund, K.A. Williams, S. Fang, K.R. Subbaswamy, M. Menon, A. Thess, R.E. Smalley, G. Dresselhaus and M.S. Dresselhaus, *Science* **275**, 187 (1997).

11) A. M. Rao, P. C. Eklund, S. Bandow, A. Thess, and R. E. Smalley, *Nature* **388**, 257 (1997).

12) A. M. Rao, J. Chen, E. Richter, P. C. Eklund, R. C. Haddon, U. D. Venkateswaran, Y. K. Kwon, and D. Tomanek, *Phys. Rev. Lett.*, **86**, 3895-3898 (2001).

13) S. Bandow, S. Asaka, Y. Saito, A. M. Rao, L. Grigorian, E. Richter and P. C. Eklund, *Phys. Rev. Lett.* **80**, 3779 (1998).

14) R. Saito, G. Dresselhaus, and M. S. Dresselhaus, *Physical Properties of Carbon Nanotubes* (Imperial College Press, London, 1998)

15) J. Chen, H. Hui, Y. Chen, A. M. Rao, P. C. Eklund, and R. C. Haddon, *Science* **282**, 95 (1998); J. Chen, A. M. Rao, S. Lyuksyutov, M. E. Itkis, M. A. Hamon, H. Hu, R. W. Cohn, P. C. Eklund, D. T. Colbert, R. E. Smalley and R. C. Haddon, J. Phys. Chem. B, **105**, 2525-2528 (2001).

16) G. Sumanasekara et al., *Phys. Rev. Lett.*, **85**, 1096 (2000).

17) G. Sumanasekara and P. C. Eklund (private comm.).

Table 1 : Comparison of the normalized derivative of ω_R with respect to pressure in SWNT samples obtained in this work and by other research groups.

ω_R (cm^{-1})	$(1/\omega_R)(d\omega/dP)$ (TPa^{-1})	vdW influence α	Material	Reference
190	44	28 %	s-SWNT (PLV derived)	This work
183	53	34 % (not used)	PLV	[1]
172	56	⎫	EA	[3]
171	57	⎬ 37 %	EA	[4]
182	56	⎭	PLV	[5]
173	48	31 %	Buckypaper (EA derived)	[2]

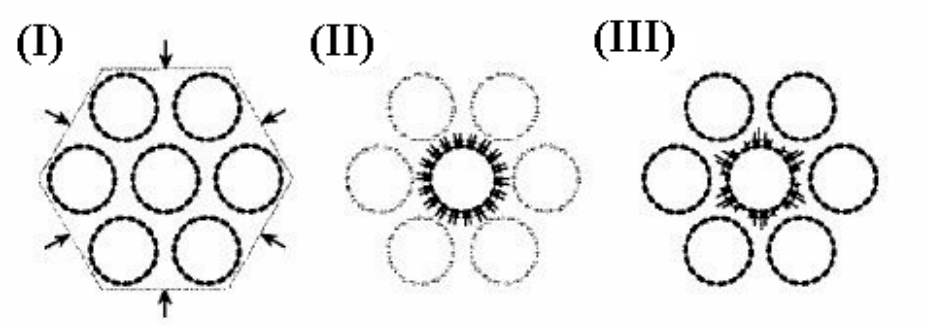

Fig. 1: Three scenarios by which the external pressure can be transmitted to bundled SWNTs (see

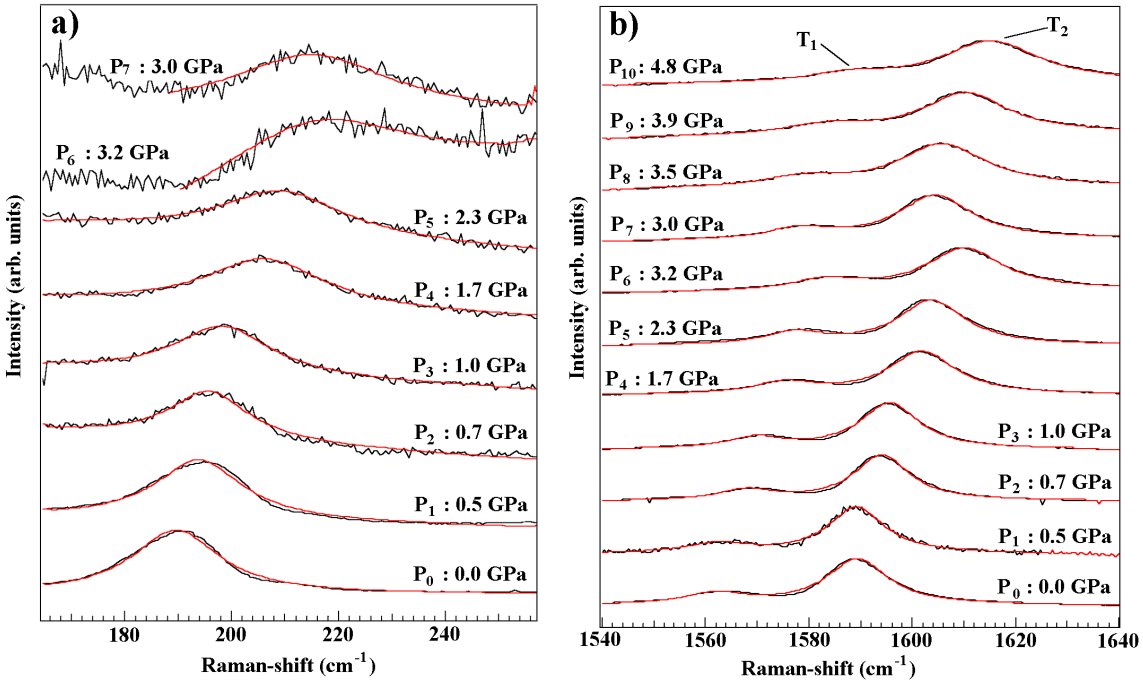

Fig. 2: Raman spectra of the radial (a) and tangential bands (b) that were observed for S-SWNTs at the indicated pressures.

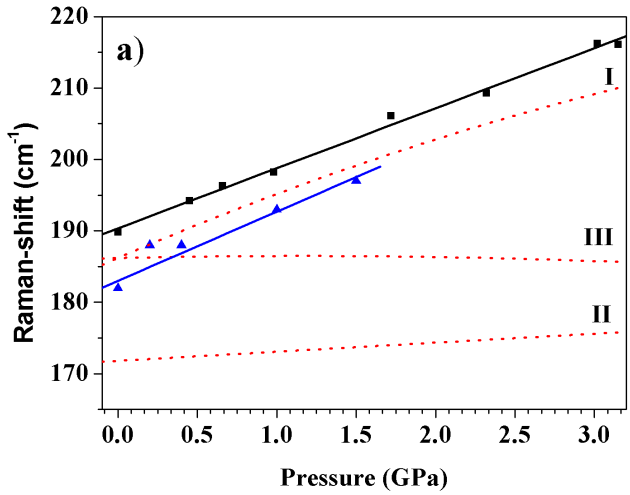

Fig. 3a : Experimentally determined pressure dependence for ω_R in S-SWNTs (squares) and bundled tubes(triangles). The solid lines represent linear fits to the data. The dashed lines are theoretical pressure dependence ofr ω_R in Models I – III (see text).

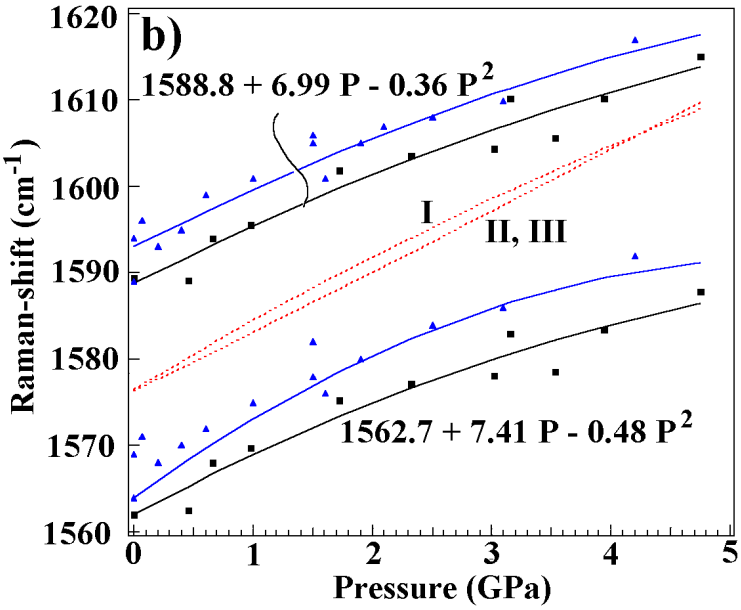

Fig. 3b : Quadratic fits (solid curves) for the two tangential mode frequencies observed in S-SWNTs (squares) and bundled tubes(triangles). The dashed lines represent model calculations discussed in Ref. 1.

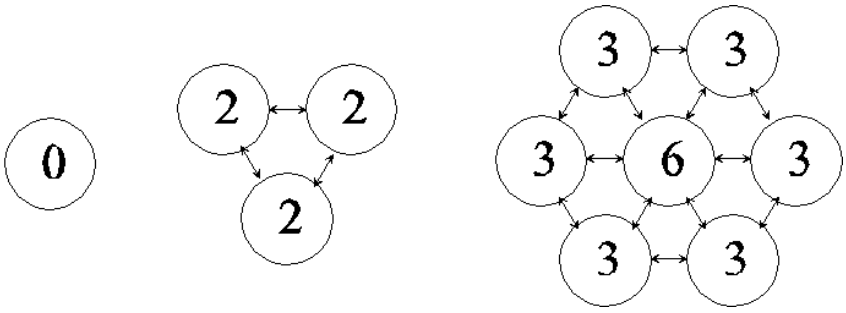

Fig. 4 : Schematic representation of small bundles found in S-SWNT samples used in this study. The numbers inside the circles represent the number of neighbors within the bundle.